


Nanometer-Scale Deformations of Berea Sandstone Under Moisture-Content Variations

Eduard Ilin^{1,*}, Maxim Marchevsky,² Irina Burkova,¹ Michael Pak,¹ and Alexey Bezryadin^{1,†}

¹*Department of Physics, University of Illinois at Urbana-Champaign, Urbana, Illinois 61801, USA*

²*Lawrence Berkeley National Laboratory, Berkley, California 94720, USA*

 (Received 19 March 2019; revised manuscript received 26 November 2019; accepted 31 January 2020; published 18 February 2020)

Sandstone mechanical stability is of key concern in projects involving injections of CO₂ in sandstone geological reservoirs, for the purpose of long-term storage. We develop a method to measure nanometer-scale deformations of sandstones in real time. We demonstrate that Berea sandstone, when hydrated, changes dimensions with a relative deformation of the order of 10⁻⁴. If the moisture content increases, sandstone samples exhibit an extension and if the moisture content decreases then the samples shrink. We also discover that, immediately after exposure to water, the sandstone temporarily shrinks, just for a few seconds, after which time a slow extension begins and continues until about half of the fluid evaporates. Such shrinkage followed by an extension is also observed when the sample is exposed to acetone, mineral spirits, or vacuum oil. The results are obtained using a high-resolution nanopositioner technique and, in independent experiments, confirmed using the technique of coda wave interferometry.

DOI: [10.1103/PhysRevApplied.13.024043](https://doi.org/10.1103/PhysRevApplied.13.024043)

I. INTRODUCTION

It is known that exposure to water can increase the volume of rock [1]. This effect differs significantly for different types of rock, with hydric dilation reaching values as high as 25% for certain clay stones, while being substantially less pronounced for other types of stones, such as granite or marble, with typical dilation values of 0.1% or less. There has been much interest in this process and a substantial amount of research activity, mostly devoted to potential degradation of mechanical properties of stones due to water dilation.

The question of the sandstone dimension change as a function of water content acquired increased significance recently due to efforts to use sandstone geological reservoirs for the long-term storage of CO₂ gas [2]. Massive geological storage of CO₂ underground causes worrisome microseismic activities [3,4], which sometimes continue even when the stored gas leaves the injection site. It is known that gas injection (as well as the extraction of natural gas) leads to massive relocations of water and brine underground, causing some areas to become dryer and some areas wetter. We propose that the observed seismic activity is due, at least in part, to water or brine relocations, causing the dimensional changes of the massive sandstone reservoirs and triggering avalanchelike events in critical tension states.

An overview of measured hydric dilatation for different types of rocks given in Ref. [1] illustrates the universal nature of this phenomenon. At the same time, there is no commonly accepted interpretation of this property, and thus, further investigations are warranted, especially because the phenomenon is so important in geological projects, as well as in any construction work involving stones. According to Ref. [1], the largest relative extension values correlate with the greater amount of clay present in the stone; thus the pronounced dilation values are associated with the swelling of clay minerals. For instance, hydric dilation measured for mudstone [5,6] reaches up to 20 mm/m, while for high-clay-content sandstone dilatation values of up to 5 mm/m are reported [7,8]; the lowest reported value appears to be 0.1 mm/m [1]. On the other hand, rocks with very small clay content still exhibit some hydric dilation, although to a much lesser extent. Even clay-free rocks, such as basalt or granite, also expand when exposed to water, which suggest a universal mechanism for the dilation. It can also be suggested that, not only the clay content, but also the porosity correlates with the hydric extension coefficient. According to Ref. [9], a larger observed expansion correlates with a greater percentage of micropores.

Significantly, the hydric dilation process is generally considered to be reversible, although the absence of measurable residual expansion after drying out does not prevent a possible loss of compressive strength, as observed in some stones [10–12]. Here, we report that the dimensions of the sample appear slightly reduced after complete

*eduard@illinois.edu

†bezryadi@illinois.edu

drying of the sample. Thus, we present evidence that the cycle of wetting and drying is not completely reversible in terms of the sample dimensions and mechanical strength. Such observed nanometer-scale changes of the dimensions can accumulate in geological settings and be a potential cause of the microseismic activity.

It is also demonstrated, in a series of experiments, that nanometer-scale pores (nanopores) play a defining role in certain situations. For example, if liquid condensation is considered, the capillary forces generated by nanopores are important [13–16].

There are no previous reports on experiments to measure the liquid-induced dimension-change effect down to nanometer-scale precision of Berea Sandstone, in real time. Such a phenomenon of fast and short-time contraction upon saturation with liquids, which we report here, has not been reported previously. Our experiments are done on small samples, but we expect that same phenomena can occur and be even more pronounced on the geological scale.

II. EXPERIMENT

We investigate expansion and contraction of sandstone samples upon saturation with polar solvents (water and acetone) and nonpolar solvents (mineral spirits and vacuum oil).

Test samples of $25 \times 8 \times 3 \text{ mm}^3$ are cut out of a large $100 \times 100 \times 20 \text{ mm}^3$ sample and rinsed. This rock, quarried from Berea, Ohio, is a fine-grained sandstone composed mainly (approximately 95% of solid volume) of subrounded to rounded quartz grains. Other constituent minerals include kaolinite (2%), microcline (1.5%), and muscovite (1.2%) [17–19]. The sandstone sample is mounted on the stable frame of a nanopositioner stage (Fig. 1).

The sensitive part of the apparatus is a controllable break junction [20,21] between two gold foils. One gold foil with dimensions of $14 \times 3.5 \times 0.1 \text{ mm}^3$ is attached to the sandstone sample, while the second gold foil of similar dimensions is mounted on the moving part of the nanopositioner stage (Fig. 1). The distance between the holder of the sample and the point where the gold foil is attached to the sample is about 13–18 mm. This distance is used as the effective length of the sample, when calculating the relative extension. The moving part of the stage is controlled by a piezopositioner (Piezoconcept), which has a range of $30 \text{ }\mu\text{m}$ for the total range of the control voltage of 10 V. The electrical resistance between the gold foils is monitored continuously during the experiment. A feedback mechanism is employed to maintain a constant electrical resistance of the break junction between the two gold foils. Using the piezopositioner, the mechanism pushes the foils closer to each other, if the electrical resistance between them increases, and pulls the gold foils apart from each other, if the electrical resistance between them decreases

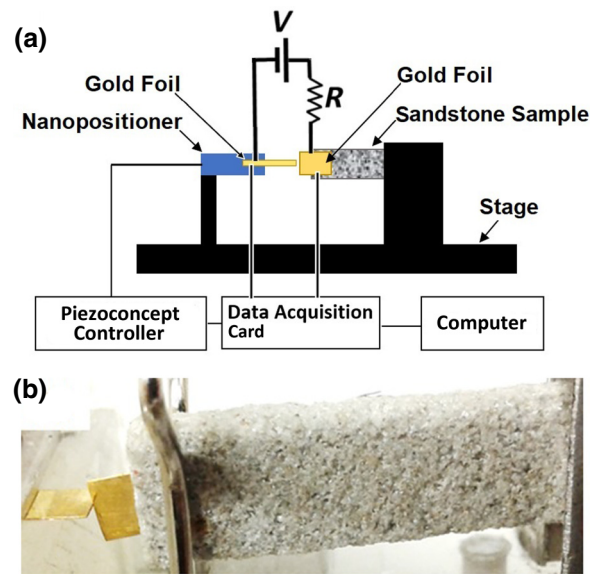


FIG. 1. (a) Schematic of the experimental setup. The setup includes two gold foils forming a break junction, i.e., contact with a mechanically controllable resistance. The left one is rigidly fixed to the moving part of the piezo-controlled nanopositioner stage of the apparatus, while the right foil is rigidly fixed to a Berea sandstone sample. It can push the sample in the horizontal direction with the precision of a few nanometers. R is a standard resistor of $1 \text{ M}\Omega$. The voltage that needs to be applied to the Piezoconcept controller, to keep the contact resistance unchanged, is proportional to the extension of the sample. (b) Photograph of the setup. Two gold foils, in contact with each other, are visible on the left. One of the gold foils is attached to the sandstone sample, which is visible at the center.

with respect to a set value. If the feedback mechanism is activated, the magnitude of the shift of the gold foil always corresponds to the magnitude of the change of the sample length, and the direction of the displacement of the gold foil is opposite to the direction of the deformation of the sandstone sample. In other words, since the device is programmed to keep the contact resistance between the pair of the gold foils constant (Fig. 1), the shifts generated by the piezopositioner are exactly equal to the changes in dimensions of the sandstone sample. The displacement of the piezopositioner is proportional to the voltage applied to it. This voltage is actually measured to determine the sample displacement.

To reduce the effect of vibrations, the piezopositioner is placed on a vibration isolation table (not shown). The contact resistance between the gold foils, i.e., the resistance of the break junction, is measured using a simple electronic circuit, which provides a fixed voltage of 0.03 V (using a Tektronix PWS4205 voltage source) between the gold foils connected in series with a resistor and the voltage on the gold foils and on the resistor is, which allows an accurate calculation of the contact resistance of the break junction.

The resistor connected in series with gold foils is 1 M Ω . To control the stability of the break junction, a Piezoconcept device is used.

In our experiments, the feedback mechanism is activated and, after a delay of 5–10 min needed to verify that the system is stable in the absence of external perturbations, about 50 μ l of liquid is added and the displacement of the piezopositioner is recorded as a function of time.

The amount of added liquid is controlled by a micropipette and constitutes 50 μ l in all experiments. The liquid is always placed on the sample from above, generally taking on the order of several seconds for the liquid to soak the sample. There is no observed dependence of any measured properties on the sample positioning. In particular, it is experimentally determined that the soaking rate is not affected by placing the sample into a vessel containing the same amount of liquid as that added from the top in other experiments. Immediately preceding the experiments, all samples are dried on the surface of an Isotemp heater for the duration of 2–3 h at a temperature of 100 $^{\circ}$ C. All measurements are protected from vibrational noise. To exclude air-convection effects, the sample is placed into a closed thermoisolated chamber, which also contributes to maintaining a stable temperature during experiments. In all experiments, the temperature is maintained at 20–22 $^{\circ}$ C and the relative humidity at 60%.

Our measurements are done with polar solvents (water and acetone) and nonpolar solvents (mineral spirits and vacuum oil) at room temperature, as well as with water heated to 100 $^{\circ}$ C (very near the boiling point).

The evaporation rate of liquids is measured using an MXX-123 Denver Instrument electronic scale in separate experiments. The precision of the electronic scale is about 1 mg. We first introduce 50 μ l of liquid into the sample, immediately place it on the scale, and measure the weight over time. The measurement shows that, as the liquid evaporates, the weight drops and eventually returns to the original value, when all liquid is evaporated.

III. RESULTS

A. Hydric dilation of sandstone

After adding water at time $t = 10$ min from the start of the measurement, we record changes of linear dimensions of the sandstone sample for about 150 min (Fig. 2). When 50 μ l of water is added, the sample is completely soaked, but no excess water is observed on its surface. The sample initially exhibits a rapid contraction, which continues for about 2 min and reaches an amplitude of the order of about 400 nm. After the initial and very rapid contraction, a relatively slow expansion begins, which continues up to the maximum extension of 600 nm (measured from the original size of the sample), achieved at time $t \approx 30$ min. After this, presumably due to water evaporation, the sample starts to shrink again. As the sample reaches its original

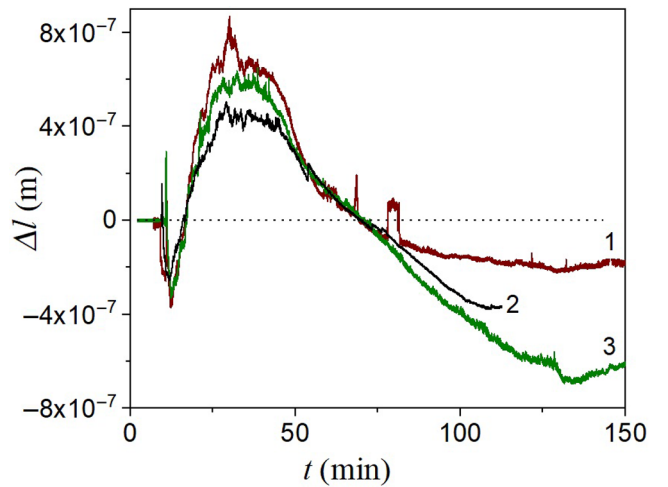


FIG. 2. Change of the length of the sandstone sample versus time. Sample is saturated with water at time $t = 10$ min. The amount of water is 50 μ l. Measurement is repeated three times, and thus, three curves are shown. Immediately before each measurement, the sample is completely dried on a hot plate (approximately 100 $^{\circ}$ C).

size, shrinkage of the sample does not stop, but continues further, so at the end of the experiment the sample reaches a somewhat smaller size than that measured before the hydration. The experiment is repeated three times, and the results are shown in Fig. 2. In what follows, we show our data on the relative scale, as in Fig. 3(a). The maximum relative extension of this Berea sandstone exhibits a peak of about 4×10^{-5} , which occurs approximately 30 min after the initial soaking of the sample with water.

In a separate experiment, the mass of the sample is measured, continuously, after 50 μ l of water is introduced into the sandstone using a micropipette. The time dependence of the measured weight of the fluid inside the sample is shown by curves 4 and 5 in Fig. 3(b), which represent the dynamics of the evaporation process. As we compare dilation curves 1, 2, and 3 and weight curves 4 and 5, in Figs. 3(a) and 3(b), we notice that the contraction process appears to continue for longer than that of the drying process. The sample continues to shrink, even after the sample weight returns to its original value measured before hydration. This observation indicates that some very small (<1 mg) amount of water may still be present, even after the mass of the sample returns to its original value. Moreover, this small amount should be concentrated at the junctions between the grains, so that the effect of this remaining moisture on the dimensions is significant. In other words, our model uses the basic idea that longer-term changes after all solvent is evaporated are caused by some metastable concentration of solvent molecules adsorbed inside the sample, most probably inside the tiny pores present in the binding material, e.g., clay. Such a view is reasonable, since one does not

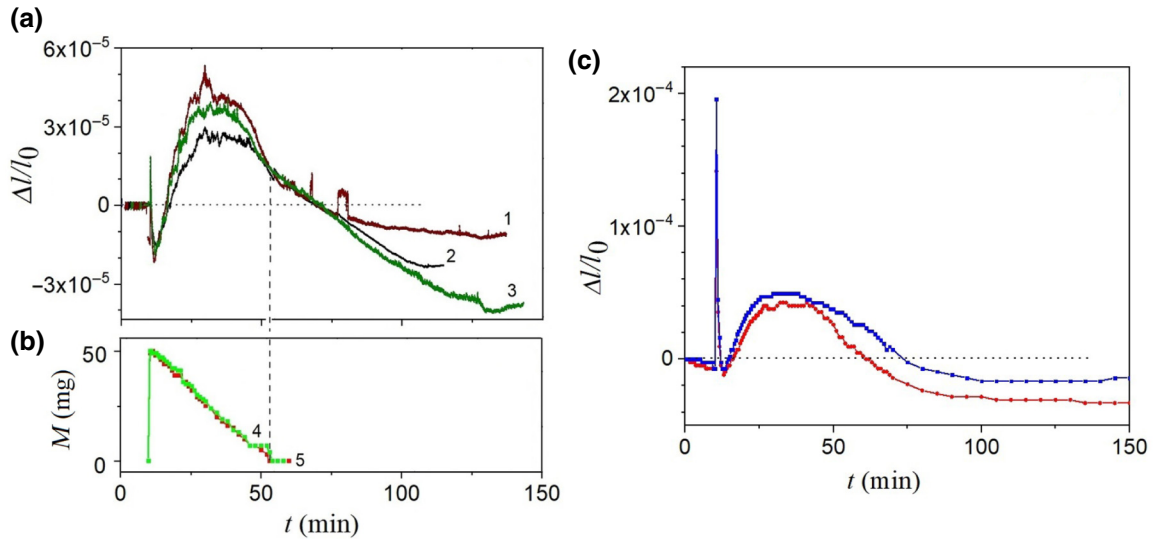


FIG. 3. (a) Relative change of linear dimension of the sandstone sample saturated with water at room temperature plotted versus time. The amount of water is $50 \mu\text{l}$. Horizontal time axes in (a) and (b) are the same. Three curves, 1, 2, and 3, represent three similar independent measurements. (b) Curves 4 and 5 represent the measured weight of water, i.e., the differential weight, inside the sample versus time. To measure these curves, $50 \mu\text{l}$ of water is introduced into the sample at $t = 10$ min and the sandstone is left on the scale to dry, as its weight is measured periodically. (c) Relative change of the sample length after saturation with water at a temperature of about 100°C .

expect many pores to be present inside the sand grains themselves. The observed approach of the additional mass to zero means that the accuracy of the weight measurement is not enough to account for the solvent molecules trapped between nanoparticles in the clay-type binding material.

In Sec. IV, we discuss a model which assumes that there is some cementing material (clay) present at the junctions between sand grains. This clay has a very small volume compared with that of all pores in the sandstone. This cementing material is made of a matrix of nanoparticles, and the nanopores in this matrix can trap water for a much longer time compared with that of large pores (“macropores”) present between sand grains in the sample. In such a model, the cementing material determines the size of the sample to a significant extent, since it is located at the contact points (the junctions) between sand grains. So, as this clay dries, the sample continues to shrink.

B. Effects of temperature on hydric dilation

In a separate experiment, we test the effect of temperature changes. For this purpose, we first heat water to near its boiling point (100°C) and then soak the sample with $50 \mu\text{l}$ of this hot water. The sample expands sharply immediately after the heated water is added; the maximum relative extension observed is about 1.9×10^{-4} [Fig. 3(c)]. After about 2 or 3 min, the sample returns to its original dimensions. Subsequent behavior of the sandstone sample is similar to that observed in hydration tests

performed with water at room temperature. The sample expands for the first 30 min, followed by contraction to initial dimensions in around 50–60 min [Fig. 3(c)]. In this test, the initial behavior of the sample is likely explained by thermal expansion due to heat transfer from added water to the sample. Our qualitative explanation (to be discussed in Sec. IV, in more detail) is that the introduced heated water comes into contact with the surface of the grains first and, of key importance, with the clay present at junctions between sand grains. The clay temperature goes up and it expands quickly. After a few minutes, the heat becomes distributed evenly and much of it goes into grains. However, since the volume of the grains is much larger than the volume of the clay, the resulting equilibrium temperature deviates only by a small amount from room temperature. By “small” we mean that the difference is much smaller than that of the average value of the absolute temperature.

We estimate linear dimensional changes of the sample using the following expression: $\Delta L = \alpha_L L \Delta T$, where α_L is the coefficient of linear thermal expansion and L is the sample length. Based on the literature [22], we assume $\alpha_L = (10.1\text{--}12.1) \times 10^{-6} \text{ K}^{-1}$. The change of the sandstone sample temperature is estimated using the heat-balance equation. The heat capacity of sandstone is $0.92 \times 10^3 \text{ J}/(\text{kg K})$ [23]. Our estimate shows that the temperature of the sample has to increase by approximately 14 K after 50 mg of hot water (100°C) is introduced into it. Taken into account this change of the sample temperature, we calculate the change of the linear dimension of the sample: $\Delta l/l_0 = (1.4\text{--}1.7) \times 10^{-4}$, whereas experiment

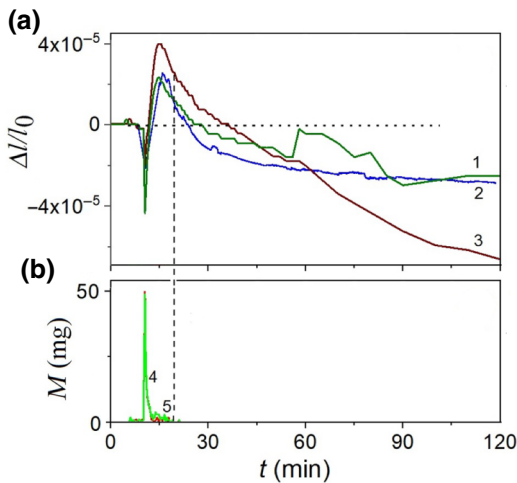


FIG. 4. (a) Relative change of linear dimension of the sandstone sample saturated with acetone at room temperature plotted versus time. Three curves, 1, 2, and 3, represent three similar independent measurements. (b) Evaporation of acetone: the time dependence of the measured weight of acetone inside the sample. The initial amount of acetone is $50 \mu\text{l}$. Horizontal time axes are the same for (a) and (b).

shows $\Delta l/l_0 = (1.4-1.9) \times 10^{-4}$ for 100°C water. Thus, the estimate is in good agreement with the measurements.

C. Acetone dilation of sandstone

Another question of interest is whether the sandstone extension, observed upon water saturation, is uniquely connected to water. Thus, similar tests are performed with acetone (Fig. 4). When acetone is introduced to the sandstone sample, the sample initially exhibits a sharp contraction, followed by a slower expansion stage, which continues for roughly 2 min until reaching the maximum size, after which the sample contracts for 60–70 min. Exposure of the sandstone to room-temperature water results in similar behavior, but the processes of expansion is faster with acetone than that with water. As with water, after acetone is evaporated, the sample continues to contract. The time dependence of the weight of the acetone inside the sample is shown by curves 4 and 5 in Fig. 4(b), which represent the dynamics of the evaporation process.

As with water, the contraction phase continues long after acetone is evaporated and the weight of the sample returns to its original value, with the precision of our scale. As with water, our explanation is that a minute amount of acetone remains trapped in the nanopores of the cementing material concentrated at the junctions between the grains and holding them together.

D. Dilation of sandstone with nonpolar liquids

To elucidate the effects of liquid polarity on sandstone dilation, additional experiments are performed with the nonpolar solvents mineral spirits and vacuum oil.

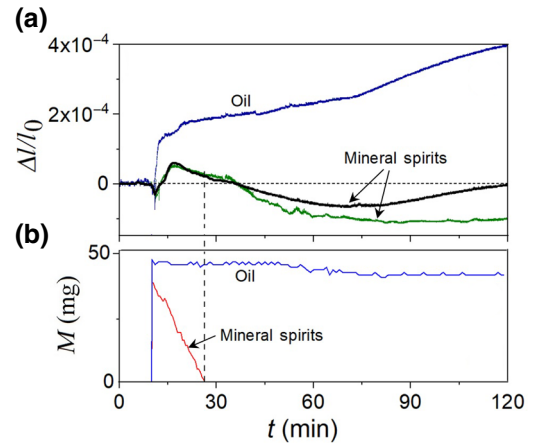


FIG. 5. (a) Relative length change of the sandstone sample plotted versus time. The sample is saturated at $t = 10$ min with either mineral spirits or vacuum machine oil at room temperature. The time axes for (a) and (b) are the same. (b) Time dependence of the weight of either mineral spirits or vacuum machine oil inside the sample determined as the current sample weight minus the weight of the sample measured before the introduction of fluid. The amount of liquid used is $50 \mu\text{l}$.

Similar to the case of polar solvents, the addition of mineral spirits leads to a short-term contraction of the sample, followed by much slower expansion [Fig. 5(a)]. The expansion stage up to the maximum size lasts for approximately 7 min, followed by contraction of the sample. This behavior is similar to that observed in water and acetone, although the expansion process with mineral spirits occurs faster than that with water, but slower than that with acetone (Table I). Similar to that with polar liquids, after complete evaporation of the solvent, contraction of the sample continued.

Another nonpolar liquid used is vacuum oil. Upon introduction of the liquid, an initial short-term contraction (approximately 1 min in duration) is followed by, at first, abrupt and then considerably slower expansion [Fig. 5(a)]. Expansion continues for the entire duration of the experiment. Weighing the sample after the addition of $50 \mu\text{l}$ of the liquid demonstrates no change to the mass of the sample in 120 min [Fig. 5(b)].

E. Acoustic measurements

We also conduct a series of experiments using an acoustic technique of coda wave interferometry (CWI) [24,25] to confirm the character of dimensional changes in the sandstone sample subjected to a moisturizing process. CWI is a technique based on ultrasound propagation, which is widely used for the detection of small local changes within an inhomogeneous medium [26]. If a sound wave induced as a short pulse passes through a complexly shaped sample with multiple internal scatters and interfaces, it travels along multiple complex trajectories exhibiting multiple

TABLE I. Liquid evaporation times and approximate durations of the observed expansions.

	Water	Acetone	Mineral spirits	Vacuum oil
Evaporation time (min)	41–45	9–9.5	16–16.5	>120
Time to maximal expansion (min)	20–25	4.7–5.9	6.7–7.8	>120
Expansion time (min)	52–57	13.8–24.5	24–28	>120

reflections along its propagation path from sample internal inhomogeneities and edges. Before being fully absorbed, the wave travels along the sample multiple times, effectively probing its interior. Such decaying waves are called coda waves [Fig. 6(a)]. There are highly repeatable, even if the medium is very disordered, if the sample does not change with time. This means that by applying the same pulse to the sample one gets the same time dependence of the resulting vibrations. Yet, if something changes within the sample, then coda waves exhibit a strong variation. Thus, the technique is a sensitive probe for small internal changes in the sample. For example, if the sample

elongates, it takes longer for the wave to pass through the sample and the pattern shifts in time towards larger times.

To test the effect of moisture on the sandstone, the sample is mechanically excited with $2.4 \mu\text{s}$ acoustic pulses applied with a piezoelectric transducer glued to the sandstone surface, and the resulting reverberating acoustic waveform is acquired by a second piezotransducer at the opposite end of the sample and recorded using a PicoScope6000 Digital USB oscilloscope. We monitor variations of the received waveform as a function of time by pulsing the sandstone sample 10 times a second and calculating the time shift corresponding to the maximum cross-correlation between the initial (reference) and subsequent waveforms. The initial waveform is recorded when the sample is dry and equilibrated at room temperature [Fig. 6(a)].

In the first test, a hot soldering iron is brought to about 2 cm from the sandstone sample and held in place, causing its surface temperature to rise by about 1 K over the 20 s time interval. The observed time-shift amplitude is -2.5×10^{-7} s (where the negative sign corresponds to a delay of the reverberating wave relative to the reference one). This is due to an increase of the time needed for the sound waves to traverse the sample.

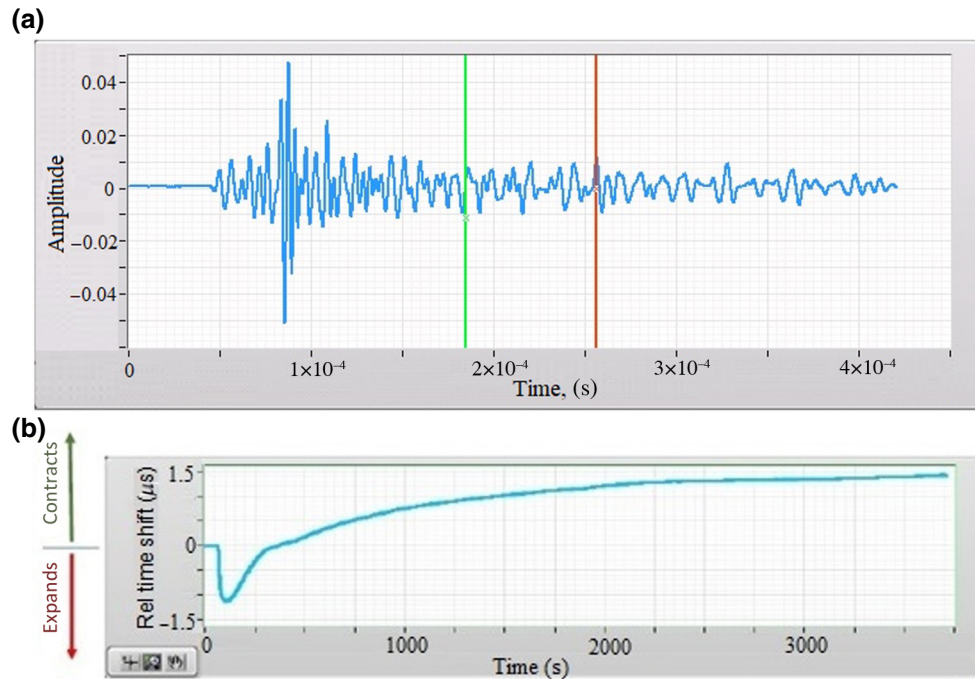


FIG. 6. Acoustic measurements of coda in acetone-soaked sandstone. (a) Snapshot showing the actual coda waveform monitored in the experiment, as well as its selected portion, which is used to compute the plot in (b). The selected portion is roughly 20 reverberation periods from the beginning of the coda, and its length is about 10 periods. As it is not exactly periodic, these numbers should be taken as a rough estimate. (b) Time shift of the reverberating sound wave compared with the reference wave measured on the dry sample. As acetone is deposited onto the sample, the time shift becomes negative. This is consistent with the expected increase of the sample dimensions. As the sample dries out, the time shift increases and eventually becomes positive, indicating sample contraction to a somewhat smaller dimensions than those of the initial ones.

In the next test, moisture-saturated air at 36 °C is blown on the sandstone surface via a straw, while the ambient air humidity is about 40%. In this experiment, the time shift is -1.2×10^{-6} over 5 s, while no noticeable surface temperature change is observed. Thus, the moisture-induced effect is nearly an order of magnitude more significant than that of the thermal one. Notably, in both experiments, the time shift is positive along the time axis, corresponding to an overall increase of acoustic wave travel time. In the first experiment, we associate this increase with the thermal softening of the sandstone Young's modulus that reduces sound velocity, while in the second experiment the moisture-driven volume expansion of the sample causes accumulation of the time delay in the reverberating wave. In the first experiment, the time shift is fully reversible and returns to a near-zero value, when the sample returns to uniform ambient temperature. In the second test with high-humidity air, the time shift decreases in amplitude as the sample is drying and approaches zero. Then the time shift changes the sign and saturates at a slightly positive value, suggesting that the sample develops a residual shrinkage, similar to the experiments involving nanometer-scale direct measurements, as discussed above.

This effect is confirmed in the third experiment, where a drop of acetone is deposited on the sample. The result [Fig. 6(b)] reproduces the general dimensional change dependence shown in Fig. 2 of the paper quite well: expansion is followed by contraction and shrinkage relative to initial dimensions. The only notable difference is the absence of the initial contraction “spike” upon introduction of the liquid. It appears that the sample remains contracted indefinitely and never returns to the original state.

IV. DISCUSSION

Our experimental techniques appear to reliably measure dimensional changes with a relative deformation of the order of 10^{-4} , and with an absolute resolution of about 10 nm or better, depending on the levels of vibrations, voltage control, and temperature stability. The measured expansion is generally consistent with previously observed results for sandstone [1]. However, there are several findings to discuss.

One such observation is the aftereffect, which is shrinkage of the sample relative to its original size after complete desiccation. Additionally, there is a notable mismatch between the timing of desiccation observed by monitoring the weight of the sample versus changes of the sample size. The dimensional changes appear to continue considerably longer in time after the drying process, as measured through the weight change, appears to be completed. We propose the following simple explanation for this observation. According to Ghurcher *et al.* [27], the composition of Berea sandstone is approximately 85%–95% of quartz, 6%–8% clay, and 1%–2% dolomite. The sandstone we use

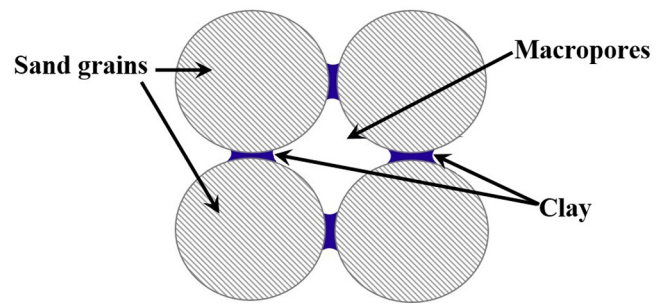


FIG. 7. Schematic representation of sandstone microscopic structure. Typical dimensions of sand grains and macropores between them are of the order of 100 μm . The “nanopores” are present inside clay (blue); they are not shown explicitly in the drawing. In our sandstone, the volume of clay (blue) is much smaller than the volume of the macropores (white) present between sand grains.

contains 2% kaolinite [17–19]. The bulk of pore space in sandstone consists of open space between the individual grains of sand forming the sandstone (Figs. 7 and 8). These pores are relatively large, since the grain size is of the order of 100 μm (Fig. 8). This is consistent with previously published data [28]. These macropores are well interconnected and are easily and quickly filled with water immediately (in the order of a few seconds in our case, because of the mm sample size in our experiment) after soaking, while water is also removed from this pore space relatively quickly when the sample is dried [over a time of approximately 53 min, according to Figs. 3(a) and 3(b)]. Due to the large size of these pores (Figs. 7 and 8), the presence of water contributes very little to the hydric expansion of the sample. Another type of pores is present in the cement material (clay) to glue the sand grains together [29,30] (marked “Clay” in Fig. 7).

In Fig. 7, the volume of the clay (blue) is illustrated as being much smaller than the volume of the macropores. It can be seen from the micrographs in Fig. 8 that the micropores between individual sand grains are much larger in size than the cementing elements of clay. Micropores are estimated [17] to be only 2% of the volume of the macropores (shown as white regions in Fig. 7). This clay also has pores with a much smaller size [30] that are called nanopores, since their dimensions, defined by the dimensions of typical clay particles, are in the nanometer range [30,31] [Figs. 8(d)–8(f)]. While nanopores occupy a much smaller volume, it is the penetration of water into these pores that primarily causes the hydric expansion of sandstone, because clay serves as a sort of glue connecting the sand gains [29]. Thus, if the clay expands, the sample expands by the same amount. The mechanism of clay expansion is related to the small size of clay-forming particles, which is of the order of a micrometer or less. Because of this small size, water molecules adhere to surface of clay

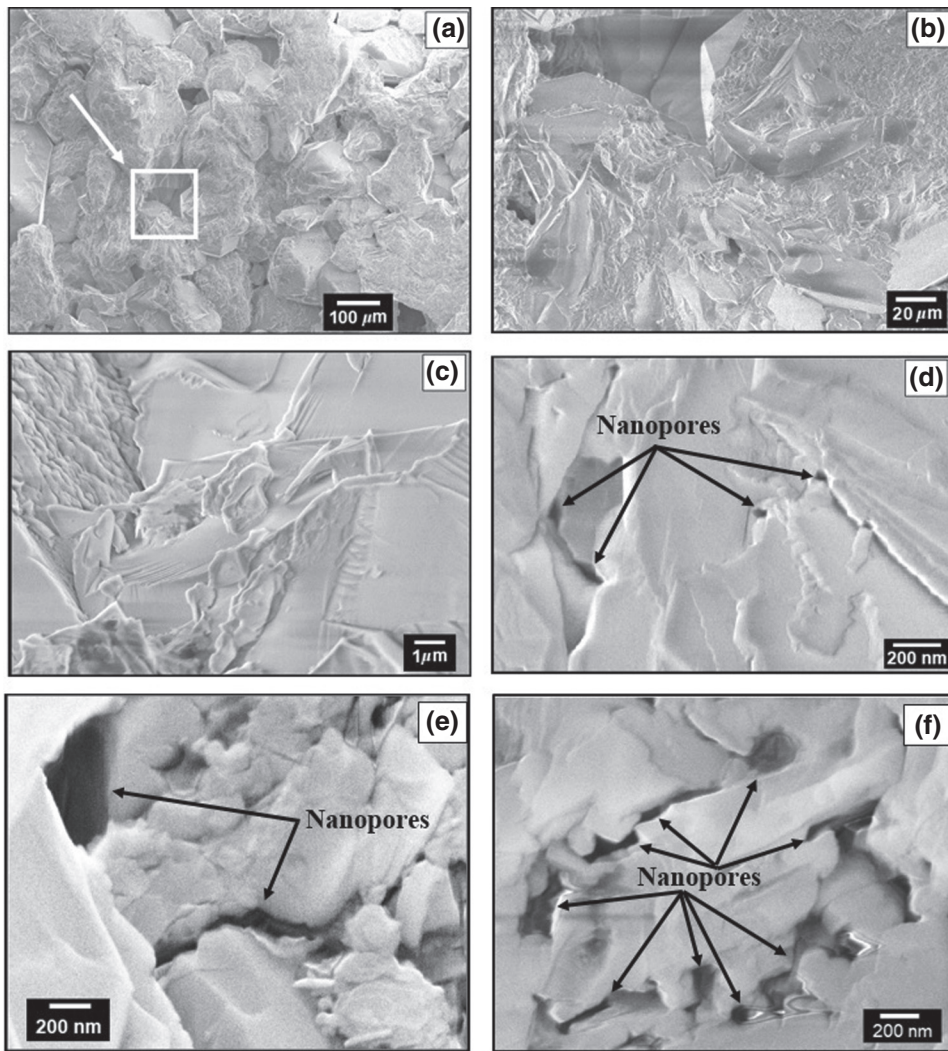


FIG. 8. Example micrographs of the sandstone surface obtained by a scanning electron microscope with different magnification. Images (b)–(f) are magnifications of the area enclosed in a square in (a). Nanopores are marked by arrows in (d)–(f). The highest magnification image (e) shows very pronounced nanopores, which appear as black areas. Another example of nanopores is given in (f); they are indicated by arrows.

particles and push them apart. Even a single layer of water molecules can produce a significant expansion. The size of the water molecule is about 0.3 nm. Thus, if the particles of clay are 100 nm in size [30,31], the relative expansion of the clay interlayers would be 0.003. Since the size of clay regions may be about 3% of the size of the sand grains, a rough estimate for the sample relative extension in this case is 0.0001, which matches the results provided above. Thus, our suggestion is to explain the observed extension by the penetration of a small amount of water between the clay particles (or clay layers), in an amount of possibly just one or a few layers of water molecules. Such a small amount appears to produce noticeable results, since the clay particles are very small. Each particle of clay is surrounded by water, and thus, clay particles are pulled apart. Of course, this mechanism is universal and would apply to any liquid that wets the surface of clay particles. Thus, it works with acetone, mineral spirits, and vacuum oil, for example, as we have reported above.

In particular, the structure of kaolinite, which might be present between the grains [17–19], is composed of

silicate sheets (Si_2O_5) bonded to gibbsite layers [aluminum oxide and hydroxide layers ($\text{Al}_2(\text{OH})_4$) [32,33]]. Silica and gibbsite sheets are held together by hydrogen bonding between the oxygen atoms at the tips of the silica sheet and the hydroxyl ions of the alumina sheet, forming the common interface between the two sheets. Hydration affects the immediate surroundings of these ions, leading to changes of intersheet physical dimensions because hydrogen bonding is affected [34].

On the other hand, the grains are made of nonporous quartz, so they do not expand by themselves. It also takes substantially more time to rid these small clay nanopores of water in the drying process [35]. This is consistent with the observed time dependences of hydric expansion and hydration (by mass) processes shown in Figs. 3(a) and 3(b). Most added liquid quickly penetrates the large pores, but it has no immediate effect on the sample size. A small amount of liquid slowly begins to penetrate the clay nanopores, causing expansion, while much larger amounts of liquid are already leaving the sample in the drying process [36]. After around 25 min, water penetrates the

nanopores in the clay and the sample shows maximum extension. At this time, as shown by sample-weight monitoring [Figs. 3(a) and 3(b)], about 50% of water filling the large macropores is evaporated, and some empty spaces appear in the pores of the sample. Thus, water trapped in the clay nanopores begins to evaporate into partially empty macropores between sand grains [37] and so the sample starts to shrink. It takes much longer for water to leave the clay nanopores [38], so the sample exhibits an overall dimension decrease over a long time, of the order of 100 min. Apparently, such flashing of the nanopores in the clay cementing material causes some removal of its constituents, so a small aftereffect is observed, which means that, after complete drying, the size of the sample is slightly smaller than that of the original size measured before hydration.

The initial very rapid change of the dimensions of the rock upon injection of liquid is more difficult to explain. We speculate that this effect might be temperature related, since its duration coincides with the duration of the initial expansion effect of hot water, which is shown in Fig. 3(c). Compare, for example, the initial expansion peak in Fig. 3(a) and the peak observed in the experiments where the sample is saturated with hot, about 100 °C, water, as shown in Fig. 3(c). The duration of the initial dimensional change is of the same order of magnitude. Thus, a thermal initial effect appears plausible. Another possible explanation is that the capillary forces are responsible for the initial contraction, as the fluid penetrates the sample. We believe that this explanation is less probable, since water penetrates the sample much faster, as observed visually because the sample changes color when wet.

V. CONCLUSIONS

We employ a nanopositioner in combination with an electrical break junction to measure minute changes in the linear dimensions of sandstones at the nanometer scale in real time. This sensitive technique is applied to study small changes of the dimensions of sandstones as they are saturated with polar solvents (water and acetone) and nonpolar solvents (mineral spirits and vacuum oil). We find that, after Berea sandstone is soaked with water, its length increases over a timescale of about 25 min. The extension is not irreversible. On the contrary, as water (or acetone and mineral spirits) evaporates from the sample, its length decreases again, reaching a value slightly smaller than that of the original size. Two unexpected effects are revealed. The first one is the apparent continued contraction of the samples, even after all water is evaporated. The time span of water evaporation is determined by weighing the sample. The weight returns to its original value after approximately 52 min (in experiments with water). Surprisingly, the reduction of the sample dimensions continues further, and, as drying of the sample is

continued, its dimensions are reduced to below the original value.

To explain this observation, we propose a model that assumes that the clay cementing sand grains together into a rigid matrix contains nanopores. It takes a much longer time to fill these clay nanopores with water, namely, about 25 min in our samples. By our estimate, these nanopores are so small that even a single layer of water molecules penetrating into them would push clay nanoparticles apart and contribute enough extension to the entire sandstone sample that it would match our experimentally observed extensions. Also, when the bulk of water is evaporated and the weight of the sample appears to return, within experimental precision, to the initial weight, some water might still be present in the clay nanopores. Eventually, all of it evaporates, but this takes a significantly longer time. Water flashing possibly changes the internal structure and composition of the clay nanopores, and thus, causes the observed small reduction of the sample dimension after each wetting-drying cycle.

ACKNOWLEDGMENTS

This work is supported as part of the Center for Geologic Storage of CO₂, an Energy Frontier Research Center funded by the U.S. Department of Energy, Office of Science, Basic Energy Sciences under award number DE-SC0012504. The authors would like to thank S. Frailey and J.S. Popovics for useful discussions.

-
- [1] Siegfried Siegesmund and Rolf Snethlage (editors), *Stone in Architecture. Properties, Durability*, Fourth Edition (Springer, Heidelberg Dordrecht London New York, 2011).
 - [2] D. N. Espinoza, S. H. Kim, and J. C. Santamarina, CO₂ geological storage — geotechnical implications, *KSCE J. Civ. Eng.* **15**, 707 (2011).
 - [3] B. P. Goertz-Allmann, S. J. Gibbons, V. Oye, R. Bauer, and R. Will, Characterization of induced seismicity patterns derived from internal structure in event clusters, *J. Geophys. Res. Solid Earth* **122**, 3875 (2017).
 - [4] A. Klovov and B. Hardage, Seismic characterization and monitoring of a deep CO₂ storage reservoir with 3D VSP using direct shear waves, *J. Petroleum Sci. Eng.* **155**, 109 (2017).
 - [5] F. T. Madsen, Quelldruckmessungen an tongesteinen und berechnung des quelldrucks nach der DLVO-theorie. Mitt institutes für grundbau und bodenmechanik, ETH Zürich **108**, 1 (1976).
 - [6] F. T. Madsen and R. Nüesch, Langzeitquellverhalten von tongesteinen und tonigen sulfatgesteinen. Mitt institutes für grundbau und bodenmechanik, ETH Zürich **140**, 1 (1990).
 - [7] H. Schuh, *Physikalische Eigenschaften von Sandsteinen und Ihren Verwitterten Oberflächen* (Münchner Geowiss Abh (B), Verlag Dr. Friedrich Pfeil, Munich, 1987).
 - [8] R. Snethlage and E. Wendler, in *Saving our Architectural Heritage, the Conservation of Historic Stone Structures*,

- Dahlem Workshop Reports ES20, edited by Baer N., Snethlage R. (Wiley, Chichester, 1997).
- [9] N. Stockhausen, *Die Dilatation Hochporöser Festkörper Bei Wasseraufnahme und Eisbildung* (Diss. Fak. Bauingenieur und Vermessungswesen, TU München, 1981).
- [10] D. M. Morales, E. Jahns, J. Ruedrich, P. Oyhantcabal, and S. Siegesmund, The impact on partial water saturation in rock strength: An experimental study on sandstone, *Z. dt. Ges Geowiss* **158**, 869 (2007).
- [11] J. Ruedrich, T. Bartelsen, R. Dohrmann, and S. Siegesmund, Moisture expansion as a deterioration factor for sandstone used in buildings, *Environ. Earth. Sci.* **63**, 1545 (2011).
- [12] L. Yinlong, W. Lianguo, and W. Jun, Experimental study of the influence of water and temperature on the mechanical behavior of mudstone and sandstone, *Bull. Eng. Geol. Environ.* **76**, 645 (2017).
- [13] A. Al-Yaseri, Y. Zhang, M. Ghasemzian, M. Sarmadivaleh, M. Lebedev, H. Roshan, and S. Iglauer, Permeability evolution in sandstone Due to CO₂ injection, *Energy Fuels* **31**, 12390 (2017).
- [14] O. Vincent, B. Marguet, and A. D. Stroock, Imbibition triggered by capillary condensation in nanopores, *Langmuir* **33**, 1655 (2017).
- [15] J. Zhong, J. Riordon, S. H. Zandavi, Y. Xu, A. H. Persad, F. Mostowfi, and D. Sinton, Capillary condensation in 8nm deep channels, *J. Phys. Chem. Lett.* **9**, 497 (2018).
- [16] M. Kang, E. Perfect, C. L. Cheng, H. Z. Bilheux, M. Gragg, D. M. Wright, J. M. Lamanna, J. Horita, and J. M. Warren, Diffusivity and sorptivity of Berea sandstone determined using neutron radiography, *Vadose Zone J.* **12**, 0135 (2013).
- [17] A. Tarokh, R. Y. Makhnenko, K. Kim, X. Zhu, J. S. Popovics, B. Segvic, and D. E. Sweet, Influence of CO₂ injection on the poromechanical response of Berea sandstone, Under Review in *Int. J. Greenhouse Gas Control* (2019).
- [18] R. Y. Makhnenko and J. F. Labuz, Elastic and inelastic deformation of fluid-saturated rock, *Phil. Trans. R. Soc. A* **374**, 20150422 (2016).
- [19] R. Y. Makhnenko and Y. Y. Podladchikov, Experimental poroviscoelasticity of common sedimentary rocks, *J. Geophys. Res.: Solid Earth* **123**, 7586 (2018).
- [20] J. J. Parks, A. R. Champagne, G. R. Hutchison, S. Flores-Torres, H. D. Abruña, and D. C. Ralph, Tuning the Kondo Effect with a Mechanically Controllable Break Junction, *Phys. Rev. Lett.* **99**, 026601 (2007).
- [21] D. Xiang, H. Jeong, T. Lee, and D. Mayer, Mechanically controllable break junctions for molecular electronics, *Adv. Mater.* **25**, 4845 (2013).
- [22] Y. Chung and H.-C. Shin, Characterization of the coefficient of thermal expansion and its effect on the performance of Portland cement concrete pavements, *Can. J. Civ. Eng.* **38**, 175 (2011).
- [23] L. Eppelbaum, I. Kutasov, and A. Pilchin, *Applied Geothermics, Lecture Notes in Earth System Sciences* (Springer-Verlag, Berlin Heidelberg), pp. 751 (107), 2014.
- [24] R. L. Weaver and O. I. Lobkis, Temperature dependence of diffuse field phase, *Ultrasonics* **38**, 491 (2000).
- [25] C. Pacheco and R. Sneider, Time-lapse travel time change of multiply scattered acoustic waves, *J. Acoust. Soc. Am.* **118**, 1300 (2005).
- [26] G. Renaud, J. Rivière, P.-Y. Le Bas, and P. A. Johnson, Hysteretic nonlinear elasticity of Berea sandstone at low-vibrational strain revealed by dynamic acousto-elastic testing, *Geophys. Res. Lett.* **40**, 715 (2013).
- [27] P. L. Churcher, P. R. French, J. G. Shaw, and L. L. Schramm, in *This Paper was Prepared for Presentation at the SPE International Symposium on Oilfield Chemistry Held in Anaheim*, February 20-22, 1991, California.
- [28] P. L. Churcher, P. R. French, J. C. Shaw, and L. L. Schramm, in *SPE International Symposium*, February 20-22, 1991, California.
- [29] S. P. Mordensky, K. Rabjohns, A. Harris, A. E. Lieuallen, and C. Verba, Characterization of the Oriskany and Berea Sandstones: Evaluating Biogeochemical Reactions of Potential Sandstone-Hydraulic Fracturing Fluid Interaction. NETL-TRS13-2016. NETL Technical Report Series. U.S. Department of Energy, National Energy Technology Laboratory, Albany, OR, 2016.
- [30] R. Kareem, P. Cubillas, J. Gluyas, L. Bowen, S. Hillier, and H. C. Greenwell, Multi-technique approach to the petrophysical characterization of Berea sandstone core plugs (Cleveland Quarries, USA), *J. Pet. Sci. Eng.* **149**, 436 (2017).
- [31] Philip H. Nelson, Pore-throat sizes in sandstones, tight sandstones, and shales, *AAPG Bull.* **93**, 329 (2009).
- [32] D. L. Bish, Rietveld refinement of the kaolinite structure at 1.5K, *Clays Clay Miner.* **41**, 738 (1993).
- [33] L. Benco, D. Tunega, J. Hafner, and H. Lischka, Upper limit of the O-H...O hydrogen bond. Ab initio study of the kaolinite structure, *J. Phys. Chem. B* **105**, 10812 (2001).
- [34] Jun Chen, Fan-fei Min, Ling-yun Liu, and Chun-fu Liu, Mechanism research on surface hydration of kaolinite, insights from DFT and MD simulations, *Appl. Surf. Sci.* **476**, 6 (2019).
- [35] D. Or, P. Lehmann, E. Shahraeeni, and N. Shokri, Advances in soil evaporation physics-A review, *Vadose Zone J.* **12**, 0163 (2013).
- [36] N. Shokri, P. Lehmann, P. Vontobel, and D. Or, Drying front and water content dynamics during evaporation from sand delineated by neutron radiography, *Water Resour. Res.* **44**, W06418 (2008).
- [37] P. Lehmann, S. Assouline, and D. Or, Characteristic lengths affecting evaporative drying of porous media, *Phys. Rev. E* **77**, 056309 (2008).
- [38] G. W. Scherer, Drying, shrinkage, and cracking of cementitious materials, *Transp. Porous Media* **110**, 311 (2015).